Environmental Science and Pollution Research (2023) 30:86072–86083
https://doi.org/10.1007/s11356-023-28185-6

RESEARCH ARTICLE

Comparative study on conventional and phase change material (PCM) based solar desalination still using low-pressure water as a heat storage medium

Rajesh Devan[1,2] · Venkata Ramanan Madhavan[2] · Vishnu Prasanna Devarajan[2]

Received: 20 December 2022 / Accepted: 5 June 2023 / Published online: 3 July 2023
© The Author(s), under exclusive licence to Springer-Verlag GmbH Germany, part of Springer Nature 2023

Abstract

Over the years, solar desalination is a renewable energy-driven method to produce freshwater from saline/ brackish water. Since solar radiation is available only in the daytime, many studies have been undertaken to store solar energy using phase change material (PCM). The aim of this study is to compare the two solar stills (still I as a conventional solar still and still II as a PCM-integrated solar still). In still II, using low-pressure water as thermal energy storage, PCM in a copper tube with a 1 liter capacity has been additionally installed than still I. Five trials have been conducted to compare the performance and yield between stills I and II, with various factors during the experiment. Remarkably, three distinct vacuum pressures − 712 mmHg (for trials 1, 2, and 3), − 690 mmHg (for trial 4), and − 660 mmHg (for trial 5) were used for the investigation to compare the performance of PCM-based solar still with conventional solar still among five trials. Finally, at a vacuum of −712 mmHg and 175 ml of water poured inside the low-pressure system, the distillate yield obtained from still II is 9.375% higher than the yield of still I.

Keywords Solar still · Desalination · Nanoparticles · Latent heat · Sensible heat · PCM · Thermal energy storage

Nomenclature

CO_2	Carbon dioxide
CH_4	Methane
FRP	Fiber reinforced plastic
PCM	Phase change material
W-c	Water temperature (°C) in conventional still
W-t	Water temperature (°C) in PCM integrated still
B-c	Basin temperature (°C) in conventional still
B-t	Basin temperature (°C) in conventional still
Gin-c	Glass inner temperature (°C) in conventional still
Gin-t	Glass inner temperature (°C) in PCM integrated still
Gout-c	Glass outer temperature (°C) in conventional still
Gout-t	Glass outer temperature (°C) in PCM integrated still
I	Solar insolation (kWh/m^2)

Introduction

Fossil fuels need to be reduced as the world shifts toward renewable energy. The utilization of fossil fuels results in the release of CO_2, CH_4, and other harmful greenhouse gasses (Devarajan and Madhavan 2022; Al-Harahsheh et al. 2018; Agrawal et al. 2017). Thus, the addition of these toxic gasses would eventually increase global warming. Also, it results in the pollution of air, land, and water. On the other hand, using renewable energy sources causes fewer environmental impacts. Renewable energy will never vanish, but fossil fuels will run out in a few decades if their consumption rate is not reduced (Bilal et al. 2019; Abd Elbar and Hassan 2019). The most harmful fossil fuel on earth is coal, whereas solar energy, one of the types of renewable energy, is not detrimental. Another advantage is that if we move towards alternative or renewable energy, the imports of fossil fuels can be reduced, especially by using solar energy, which is abundant in our country. Then, solar radiations are

Responsible Editor: Philippe Garrigues

✉ Rajesh Devan
rajesh2energy@gmail.com

[1] Panimalar Engineering College, Chennai 600 123, Tamil Nadu, India

[2] Department of Mechanical Engineering, Institute for Energy Studies, CEG–Anna University, Chennai 600 025, Tamil Nadu, India

encountered with scattering by air molecules, water vapor, and other particulates present. Due to the phenomenon of spreading in the atmosphere, solar radiation is classified into beam and diffuse radiation. Beam radiation is the normal component of solar radiation that propagates along the earth-sun line and the surface of the receiver/ receiving surface. It is also known as direct radiation. As mentioned earlier, diffuse radiation is part of solar radiation which gets scattered by aerosols and other particulates. Unlike beam radiation, it has no definite direction (Abd Elbar and Hassan 2019; Faegh, and Shafii 2017; El-Sebaii et al. 2009). Interestingly, Ansari et al. (2013) reported the desalination of brackish water using passive solar still with heat energy storage system in an effective way and Ghachem et al. (2021) investigated PCM-filled cylinders effect of the magnetic field.

A solar desalination process involves evaporating saline or brackish solutions with solar power, directly or indirectly, followed by condensation of the vapor generated. In other words, it combines humidification and dehumidification within the setup. It does not need skilled manpower, and very little maintenance is sufficient. Solar still consists of an air-tight basin. Generally, cement, concrete, or fiber-reinforced plastic (FRP) or a metal body is used for the basin. The interior part of the basin is black to improve its absorption of short-wavelength solar light due to the top cover's transmission. Glass, plastic, etc., are used to make the top cover. The blackened absorber plate gets heated and transfers most of its energy to the water mass. Some energy is lost to the ambient air through the insulation on the bottom of the solar still. Convection, evaporation, and radiation transfer heat from the water to the glass cover's inner surface (Kabeel et al. 2018a; Kabeel and Abdelgaied 2016). Water evaporated from the basin gets condensed at the inner surface of the top cover. Then it is collected at the distillate channel near the top cover's bottom end. The top cover transfers the energy absorbed from water vapor to ambient air by convection and radiation. Hence, retaining heat inside the basin is an important strategy in the solar desalination process. Interestingly, Faghiri et al. 2023 investigated the PCM melting characteristics under three different geometries by using paraffin as the PCM in a novel heat exchanger called a double spiral quality heat exchanger with two separate parts; the results show that the requirement in the radius of the inner spiral tube resulted in over capability of melt PCM at the beginning of the charging procedure but more efficiency at the final stages. In addition to this, Faghiri et al. 2021 investigated the interplay between the drop boiling and the heat extraction process from the phase change materials during impact, the impact of acetone drops into molten paraffin as a direct-contact solidification method has been experimentally explored, the maximum crater depth and width increased with both the molten paraffin temperature and the impact Weber number, according to the results.

According to the study done by Bhatti et al. 2022, the effectiveness of the heat transfer process and the overall performance of the device are significantly influenced by the thermal conductivity of the heat transfer fluids; the transfer of heat can be done using nanofluids with base fluids (such as air, water, silicon fluids, minerals, aromatic hydrocarbon fluids, propylene glycol/water composites, and synthetic refrigerants). Selimefendigil and Öztop 2022 conducted similar research on the effects of combining an elastic fin and magnetic field on the dynamics of the phase change process during the convection of nano liquids in a cylindrical reactor embedded with a bed packed with phase change material. In addition, Faghiri et al. 2022 investigated the multi-objective optimization of acetone droplet impingement on phase change material in the direct-contact discharge method. The drive of this study is to investigate the performance of conventional solar desalination and PCM incorporates solar still, using low vapor pressured water as PCM is the novelty; this analysis produced results that further justified the economic viability of the new modified solar still, particularly for seawater desalination. Ayoub and Malaeb (2014) reported costs for fuel-based brackish water and seawater desalination were thus adjusted to include unaccounted-for expenses related to environmental damage.

Similarly, our study is focused on analyzing the experimental findings to determine the best conditions for the best yield by comparison between stills I and II, by using low-pressure water used as PCM (still II) in comparison to a conventional model solar still (still I) with required operating conditions; by evaluating the performance with the hourly differences in saline water temperature, the internal and external solar still temperature differences, and the distillate yield.

Materials and experimental setup

The design and fabrication work of solar stills, PCM-filled copper tubes (low-pressure water used to store as thermal energy material), and other components has been fabricated/ purchased indigenously. Still I, a conventional single-slope, single-basin passive still, was used as the study's reference solar still for comparing the performance of PCM-integrated solar stills. Solar still II, PCM integrated (solar stills I and II have been chosen from the comparative performance test among 4 solar stills). Then, to compare the performance of stills I and II, the best and most similarly performing solar stills were chosen from 4 similar size fabricated solar stills.

Design, modeling, and fabrication of solar stills

Solar stills were designed and modeled using Solid Works 3D. The following criteria are used when designing solar

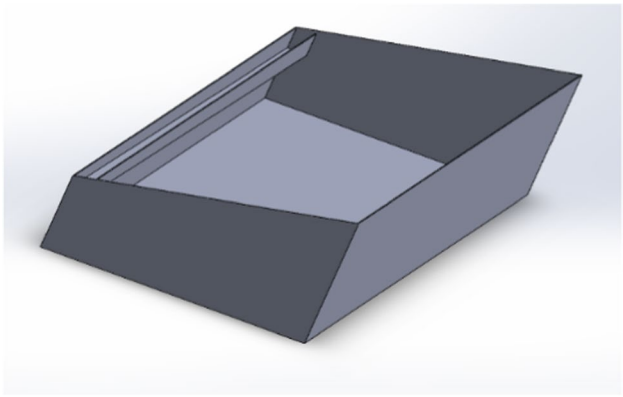

Fig. 1 Model of solar still

Fig. 2 Solar still after black painted

stills. Considered, the width and length of 0.75 m and 0.3 m respectively, with an aspect ratio of 0.4. The front wall height has less than 0.1 m since side shadow effects could decrease the still's output (Kabeel et al. 2018b) and the brine water outlet with a 1-inch pipe diameter, and the brine water inlet with a 3-inch pipe diameter, with inlet and outlet valves for opening and closing of the pipes. Thus, a depth of 0.02 m in the water has been selected (the designed basin of the solar still model is illustrated in Fig. 1). Based on the literature, the metal thickness chosen between 1 and 1.5 mm generates good results, hence 1.2 mm has been chosen. Due to structural rigidity and compactness, mild steel has been used to construct the solar stills (Kabeel et al. 2020; Yousef and Hassan 2019; Radhwan 2005). Similarly, the 4-mm glass thickness has been considered with the optimal inclination angle for the glass cover being equivalent to the location's latitude, hence a slope inclination angle of 13° has been considered. The experiment was conducted in Guindy, Chennai (Tamil Nadu, India), which is 13° latitude (Vigneswaran et al. 2019).

Four identical stills with the same frontal height and basin size were fabricated (Figs. 1, 2, and 3d). The four stills were tested to check their performance for comparison; tests were conducted after several leak tests before the final comparison test. J-type thermocouples were used to measure the temperature of the basin, the water, and the glass lid. The results of four stills by the water yield were recorded as 440 ml for still 1, 485 ml for still 2, 490 ml for still 3, and 430 ml for still 4. Finally, by considering the closest /similar performances, the best two solar stills (still II and still 3) were chosen for a comparative study between Still I (conventional solar still) and still II (PCM integrated solar still).

Subsequently, to compare the performance of still II with still I, still II has been additionally integrated with the low-pressure water-filled copper tube configuration as PCM-based solar still with a detachable type. For fabrication, a copper tube with a diameter of 1 inch was selected, which has a volume of 1 liter to hold water. The reservoir has approximately 1-m long with a valve at one end. A vacuum gauge has been fastened to the opposite end to measure the reservoir's internal pressure. The copper pipe is painted black to increase absorptivity and vacuum gauge readings in mmHg (millimeters of mercury). Since cleaning the inner tube is time-consuming and laborious, distilled water was utilized to prevent the accumulation of scale or any salt deposits inside the tube, and the water inside the setup was filled using a syringe. To prevent the water from being sucked by the vacuum pump, a separate valve setup has been connected. In addition to the fabrication work, a proper leakage test was conducted, by using nitrogen gas to check the leak after being filled, sealed, and then dipped inside a soap solution. For still II, the fabricated low-pressure water tube has been connected (shown in Fig. 3c). Copper was selected as a suitable material due to its potent thermal diffusivity (Salah, et al. 2017; Azari et al. 2013). The tube's opposite end, with two apertures on the lateral side, was utilized for water inlet, vacuum suctioning, and positioning of the vacuum gauge.

The solar still setups have been protected inside by the glass lid, and insulation was achieved by using 12-mm thick Thermorex material (Panchabikesan et al. 2019; Khan et al. 2016; Velraj et al. 1999). Silica sealant has been used to fill the gaps between the sides and bottom of the still, preventing air from entering or leaving. To measure the surrounding temperature, water temperature, basin temperature, inner glass temperature, outer glass temperature, and copper tube temperature, various thermocouples were attached. The performance of the same-sized two single-slope passive solar stills (as shown in Fig. 4) has been investigated under identical weather conditions.

Instrumentation setup and experimentation

Solar stills I and II were placed with five digital thermocouples to measure, the inner and outer temperatures of the glass cover, the water temperature, the basin temperature, and the ambient temperature. A data logger connected to a pyranometer and an anemometer were also used to measure

Fig. 3 **a**, **b** Solid works model. **c** Fabricated low-pressure system (PCM). **d** Fabricated 4 solar stills for testing

Fig. 4 Conventional (left) and PCM integrated (right) solar still

solar radiation and wind velocity, respectively. A pyranometer measures the solar irradiance that strikes a flat surface from a hemi-spherical field of view. The units were recorded in Watts per square meter (W/m^2) for irradiance. Also, the data logger has been synchronized with the pyranometer to automatically display the data in digital format, with an automatic data storage system. Thermocouples were used because of their affordability, high-temperature limits, broad temperature ranges, and robustness (Vasu et al. 2017). Both conventional and modified solar stills employ five thermocouples in each setup, where thermocouples operate according to the Seebeck effect theory (Haillot et al. 2017; Darawsheh et al. 2019; Al-Harahsheh et al. 2022). Herein, an anemometer is used to measure wind speed (Panchabikesan

Table 1 Operating conditions and output of still II for trials 1, 2, 3, 4, and 5

Parameter/properties	Operating conditions for trials 1, 2, 3, 4, and 5				
	Trial 1	Trial 2	Trial 3	Trial 4	Trial 5
Vacuum pressure (mmHg)	−712	−712	−712	−660	−690
Quantity of water in the low-pressure system (ml)	350	350	175	175	175
Water depth (cm)	5.14	3.08	3.08	3.08	3.08
The boiling point of water (°C) inside the copper tube	37	37	37	50	43

et al. 2017), the flow of air becomes impeded and moves the shaft that gauges wind speed with 1 to 25 m/s accuracy, 0.3% relative deviation at 0.2 m/s 0.01 m/s of resolution 9 V battery power. Also, vacuum gauges were used to measure pressures lower than ambient air pressure, which is utilized as the zero point, after creating a vacuum.

The experiments were conducted for 5 days (trial 1, trail 2, trial 3, trial 4, and trial 5) to compare the performance and yield of still I and still II, during the experiments the solar intensity and parameters followed for the experiments have been influenced the performance and yield.

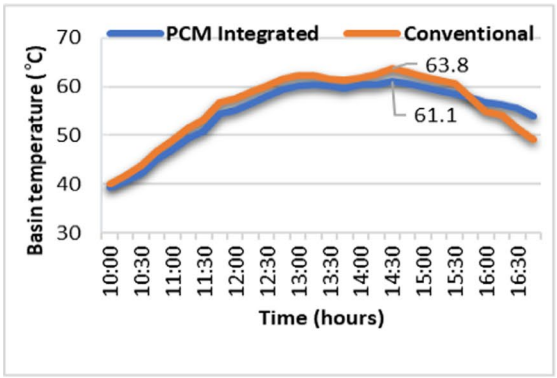

(a) Basin Temperature vs Time

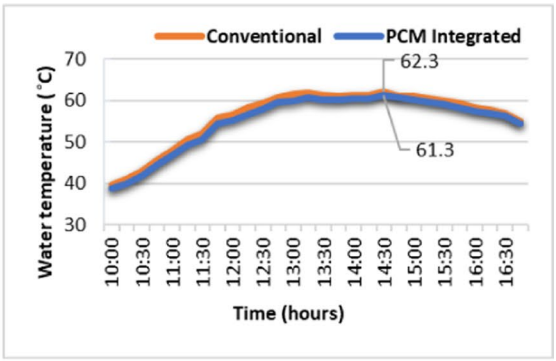

(b) Water Temperature vs Time

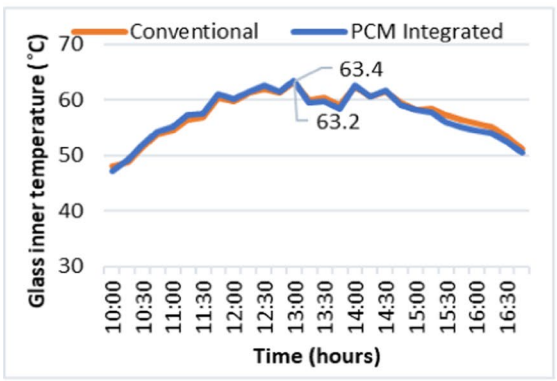

(c) Glass Inner Temperature vs Time

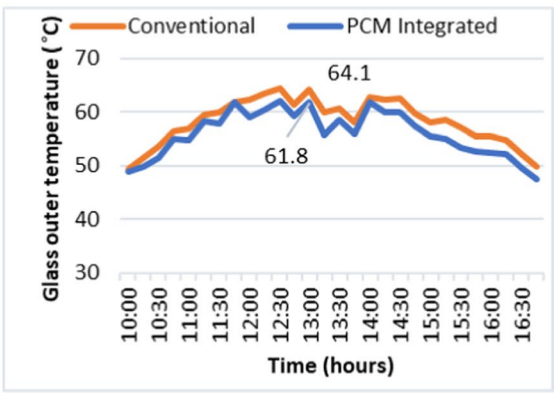

(d) Glass Outer Temperature vs Time

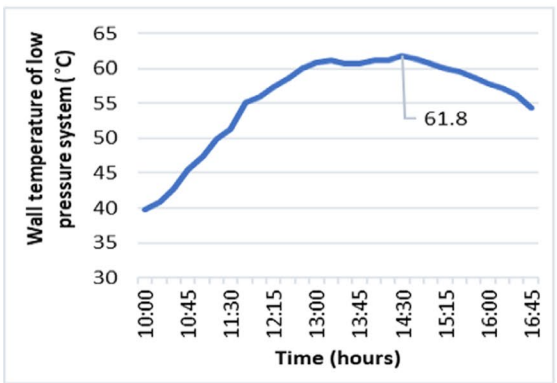

(e) Wall Temperature of Low-Pressure System vs Time

(f) Solar Intensity vs Time

Fig. 5 The experimental analyses of trial 1 (**a**–**f**)

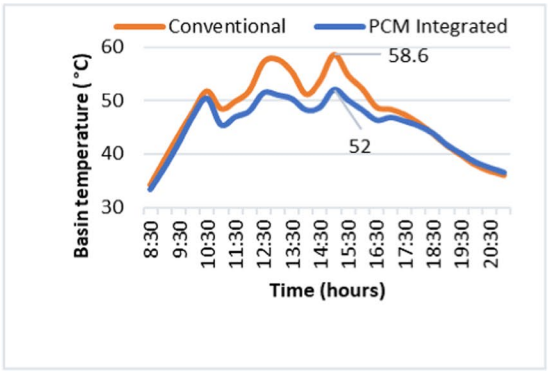

(a) Basin Temperature vs Time

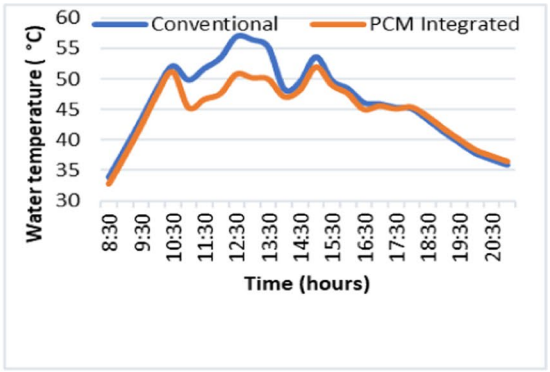

(b) Water temperature vs Time

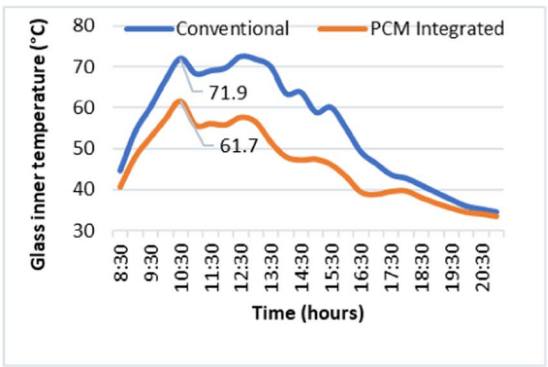

(c) Glass Inner Temperature vs Time

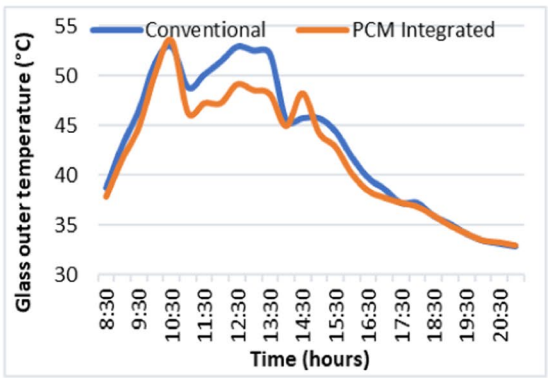

(d) Glass Outer Temperature vs Time

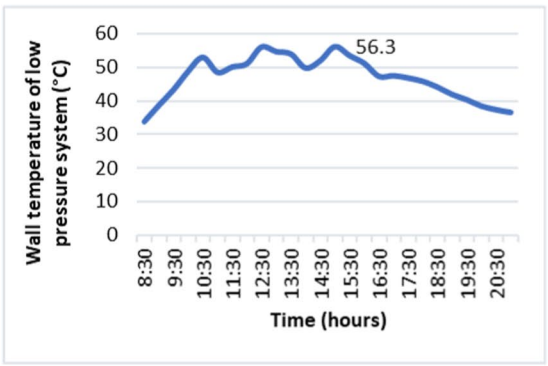

(e) Wall Temperature of Low-Pressure System vs Time

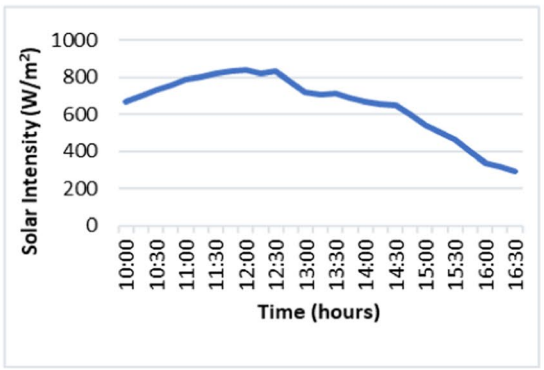

(f) Solar Intensity vs Time

Fig. 6 The experimental analyses of trial 2 (**a**–**f**)

In still II, a low-pressure copper tube PCM system has been filled with 175 ml (for trials 1, 4, and 5) and 350 ml (for trials 1 and 2) of water. Also, three distinct vacuum pressures have been selected and adjusted − 712 mmHg (for trials 1, 2, and 3), − 660 mmHg (for trial 4), and − 690 mmHg (for trial 5), with the same water depth were investigated except trial 1(water depth 5.14 cm). The operating conditions of still II for trials 1, 2, 3, 4, and 5 are shown in Table 1.

Results and discussion

The findings of the experimental analysis and yield achieved from the solar stills I and II experimental trials. Figures 5, 6, 7, 8 and 9 show the experimental analyses of the variation of basin temperature, water temperature, glass inner and outer temperatures, low-pressure system

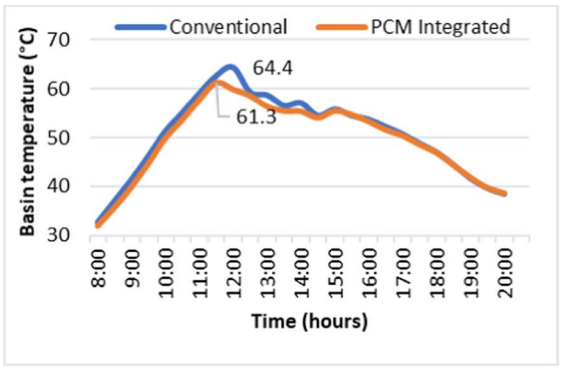

(a) Basin Temperature vs Time

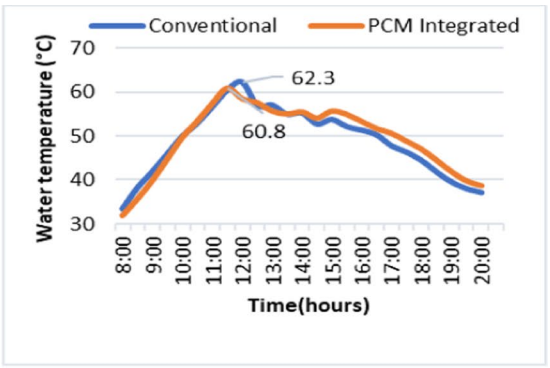

(b) Water Temperature vs Time

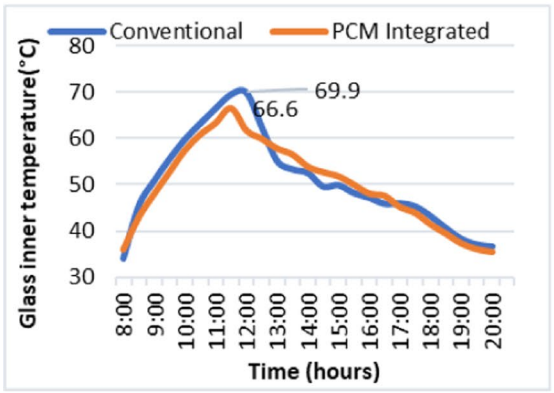

(c) Glass Inner Temperature vs Time

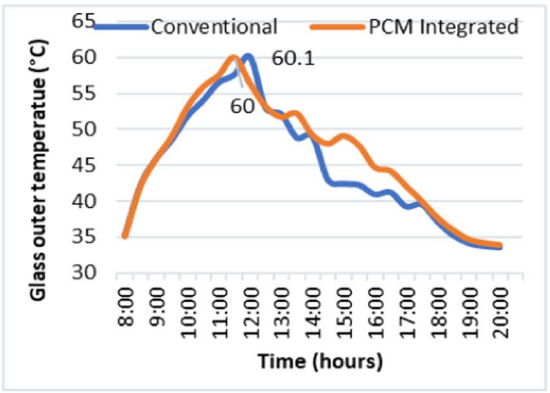

(d) Glass Outer Temperature vs Time

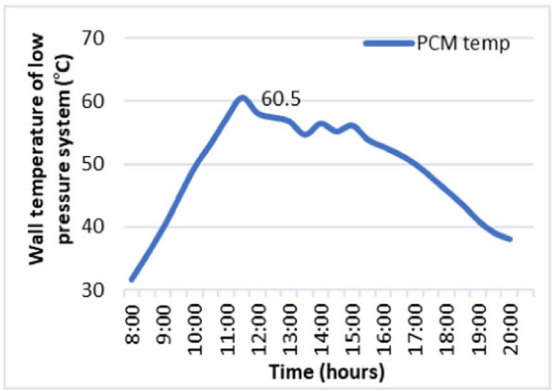

(e) Wall Temperature of Low-Pressure System vs Time

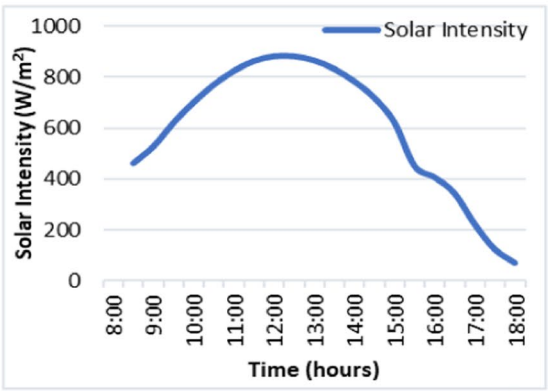

(f) Solar Intensity vs Time

Fig. 7 The experimental analyses of trial 3 (**a**–**f**)

wall temperatures, and solar intensity of five trials. The 24-h format is used to indicate time on the graphs.

Experimental analysis of five trials

The PCM-integrated solar still's basin temperature increased after 3.45 p.m. in trial 1 (as shown in Fig. 5a) compared to the conventional solar still. Basin temperature in conventional still is greater during the rest of the time (Fig. 5a). Although the water temperature in the two stills is comparable (Fig. 5b), the conventional still consistently records a higher value throughout the day. For both stills, the inner glass temperature trend appears to be identical (Fig. 5c), whereas the exterior glass temperature in both stills shows

Fig. 8 The experimental analyses of trial 4 (**a**–**f**)

a similar trend with conventional still consistently having higher values (Fig. 5d). As shown in Fig. 5e, there is little variation in the low-pressure system's wall temperature between 12.30 and 4.45 p.m. At 12.30 p.m., the sun's maximum intensity was 837 W/m^2 as shown in Fig. 5f.

Interestingly, the conventional solar basin temperature is still greater than in the PCM integrated solar still in trial 2 (Fig. 6a), from 8:00 a.m. to 5:00 p.m. The tendency appears to be the same in both stills. Similar to basin temperature, from 8.30 a.m. to 5:00 p.m., the water temperature in conventional solar stills is higher than that of PCM-integrated solar stills (Fig. 6b). In Fig. 6c, the trend of glass inner temperature is identical in both stills during the entire day. Subsequently, the glass's outside temperature pattern seems similar in both stills, just like the glass's internal temperature does (Fig. 6d). In Fig. 6e, at 3:00 p.m., the wall temperature

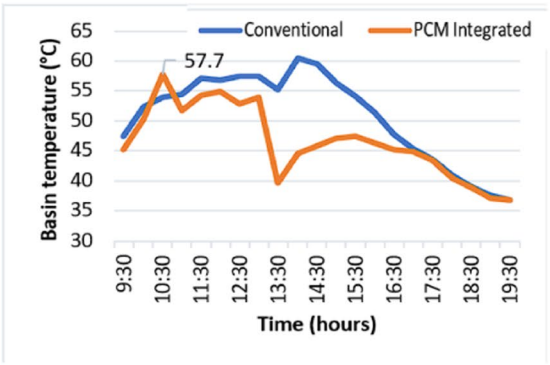

(a) Basin Temperature vs Time

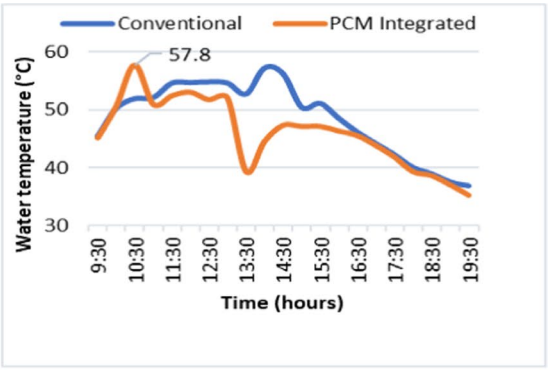

(b) Water Temperature vs Time

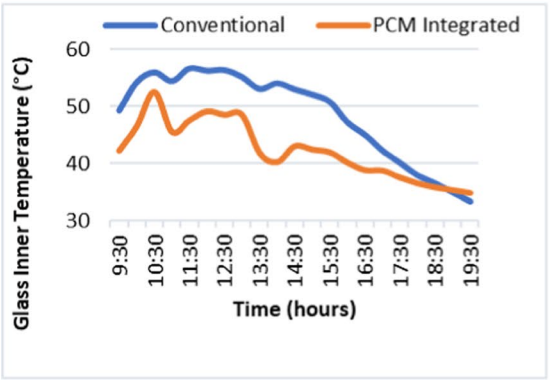

(c) Glass Inner Temperature vs Time

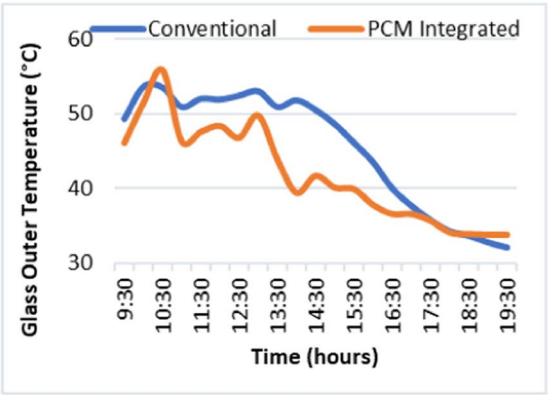

(d) Glass Outer Temperature vs Time

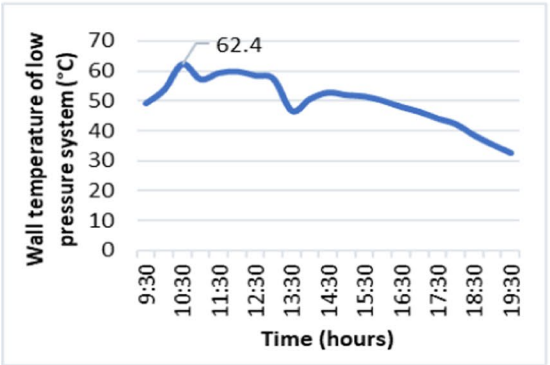

(e) Wall Temperature of low-pressure system vs Time

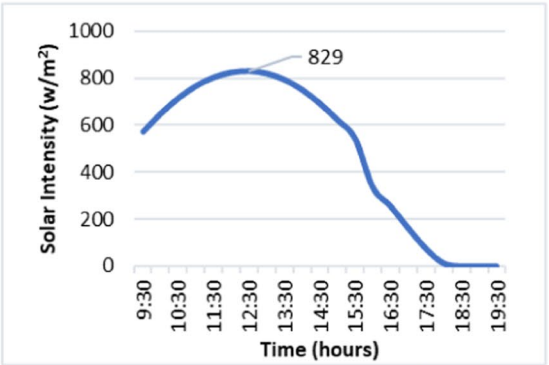

(f) Solar Intensity vs Time

Fig. 9 The experimental analyses of trial 5 (**a**–**f**)

reaches its highest point of 56.3 °C. The various solar intensities measured in trial 2 are shown in Fig. 6f. At 1:00 p.m., the most intense solar intensity was 870 W/m^2.

Remarkably, in trial 3, from 8.00 a.m. to 2.30 p.m., the basin temperature in conventional solar still is higher than in PCM integrated solar still. After 2.30 p.m., there is not much change in trend between the stills. From 2.00 to 8.00 p.m., the water temperature in PCM integrated solar still is higher than in conventional still. Up to noon, most of the time, the glass inner temperature in conventional solar still is higher when compared to PCM integrated still. From 12.00 to 4.30 p.m., the trend is reversed. Again after 5.00 p.m., the temperature in conventional still dominates PCM integrated solar still. Throughout the day, most of the time, the glass outer temperature in PCM-integrated solar still has higher than conventional solar still. The wall temperature reaches

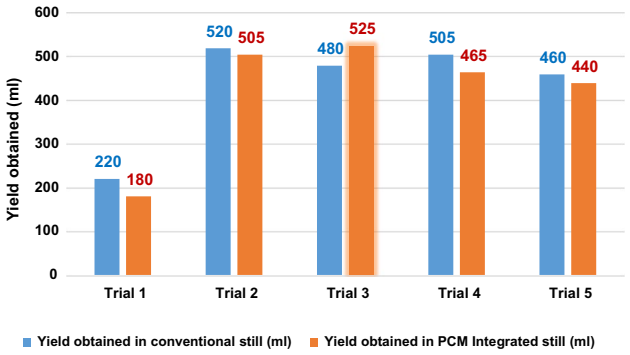

Fig. 10 Yield obtained in solar stills I and II

a maximum of 60.5 °C at 11.30 a.m. The maximum solar intensity recorded as 882 W/m^2 at noon. Representing the above details, Fig. 7 illustrates the experimental analyses of the variation of basin temperature, water temperature, glass inner and outer temperatures, low-pressure system wall temperatures, and solar intensity throughout trial three.

In trial 4, the basin temperature in the PCM integrated solar still is lower than in the conventional still throughout the entire day. The water temperature in a conventional solar still is higher from 11:00 a.m. to 5:00 p.m. than the PCM integrated solar still. The temperatures in the two stills do not differ significantly during the rest of the period. The interior glass temperature in the PCM integrated solar still is higher than in the conventional still up until 11.30 a.m. The temperature in the conventional still is higher than in the PCM integrated solar still from 11.30 a.m. to 5:00 p.m. The subsequent interval reveals a reversal of the trend. Most of the day, the glass outer temperature in conventional solar still is higher than in PCM integrated still. The wall temperature reaches a maximum of 55.95 °C at 11.00 a.m. Maximum Solar intensity has been recorded as 800 W/m^2 at 1:00 p.m. The experimental analyses by the variation of basin temperature, water temperature, glass inner temperature, glass outer temperature, low-pressure system wall temperature, and solar intensity of trial four are shown in Fig. 8.

In the case of trial 5, the basin temperature in PCM integrated solar still is lesser than in conventional still most of the time. At 1.30 p.m., 2.5 L of water were used in the PCM-integrated solar still. Thus, basin temperature in PCM integrated solar still decreases from 1.30 to 2.00 p.m. The profile is similar to the basin temperature. Therefore, the water temperature in PCM-integrated solar still drops from 1.30 to 2.00 p.m. The glass inner temperature in conventional solar still is higher than in PCM integrated solar still. In conventional solar still, the temperature of the glass's outer surface is greater, following the trend of the glass's inner temperature. At noon, the wall temperature reaches its highest point of 59.9 °C. Due to the increase of 2.5 L to the basin from 1.30 to 2.00 p.m., the wall temperature decreases. At 12:30 p.m., the sun's maximum intensity was 829 W/m^2. Figure 9 shows the experimental analyses of trial five's variations in the basin temperature, water temperature, glass inner and outer temperatures, low-pressure system wall temperature, and solar intensity.

Yield comparison of stills I and II

Considerably, the distillate yield obtained from solar stills I and II are compared (Fig. 10), concerning the yield obtained by five experimental trials, along with solar intensity, the low pressure inside the system caused the low-pressure water system as PCM, which retained the heat and accomplish the quickest time to reach the boiling point of water. It must be noted that trial one has the lowest yield because the basin was filled with more water for the experiment (water depth of 5.14 cm). Trial three results show a higher yield because of the effect of water inside the low-pressure tube on water filled in the basin. The yields for stills I and II are 480 ml and 525 ml, respectively.

Conclusion

Analysis of the effects of the variation of basin temperature, water temperature, glass inner and outer temperatures, wall temperature of the low-pressure system, and solar intensity of the five trials' results, the findings show that increasing the outside surface of the system with black paint and decreasing the amount of water have favorable effects on the performance of the solar still at certain vacuum pressure. Additionally, the productivity of the solar still is influenced by the amount of basin water. Compare with still I, the yield of still II has increased by 9.375% when 6 liters of basin water and a low-pressure system filled with 175 ml of water at − 712 mmHg. According to this study, economically cheaper PCM-based materials can be promoted to establish more solar stills in remote areas with limited water resources. The PCM-integrated solar stills are a potential strategy to improve the desalination system's overall thermal efficiency. Only socio-economic factors (cost of capital, operation, maintenance, ease of scaling up) and geographic factors (installation in remote places, availability of suitable employees) would affect choice. But, while low pressurized water use as PCM in PCM-integrated solar is still a solid choice for regions in developing countries for economic viability.

Author contribution In addition to coming up with the idea and the research of this journal all writers contributed. Mr Rajesh D, who wrote the initial draft of the research article; Mr Vishnu Prasanna D, who

worked on verifying the data; and Dr Venkata Ramanan M, who made corrections and finalized it.

Data availability Not applicable

Declarations

Ethics approval and consent to participate Not applicable

Consent for publication Not applicable

Conflict of interest The authors declare no competing interests.

References

Abd Elbar AR, Hassan H (2019) Experimental investigation on the impact of thermal energy storage on the solar still performance coupled with PV module via new integration. Sol Energy 184:584–593. https://doi.org/10.1016/j.solener.2019.04.042

Agrawal A, Rana RS, Srivastava PK (2017) Heat transfer coefficients and productivity of a single slope single basin solar still in Indian climatic condition: experimental and theoretical comparison. Resource-Efficient Technol 3(4):466–482. https://doi.org/10.1016/j.reffit.2017.05.003

Al-Harahsheh M, Abu-Arabi M, Mousa H, Alzghoul Z (2018) Solar desalination using solar still enhanced by external solar collector and PCM. Appl Therm Eng 128:1030–1040. https://doi.org/10.1016/j.applthermaleng.2017.09.073

Al-Harahsheh M, Abu-Arabi M, Ahmad M, Mousa H (2022) Self-powered solar desalination using solar still enhanced by external solar collector and phase change material. Appl Therm Eng 206:118118. https://doi.org/10.1016/j.applthermaleng.2022.118118

Ansari O, Asbik M, Bah A, Arbaoui A, Khmou A (2013) Desalination of the brackish water using a passive solar still with a heat energy storage system. Desalination 324:10–20. https://doi.org/10.1016/j.desal.2013.05.017

Ayoub GM, Malaeb L (2014) Economic feasibility of a solar still desalination system with enhanced productivity. Desalination 335(1):27–32. https://doi.org/10.1016/j.desal.2013.12.010

Azari A, Kalbasi M, Rahimi M (2013) Numerical study on the laminar convective heat transfer of alumina/water nanofluids. J Thermophys Heat Transfer 27(1):170–173. https://doi.org/10.2514/1.T3834

Bhatti MM, Öztop HF, Ellahi R (2022) Study of the magnetized hybrid nanofluid flow through a flat elastic surface with applications in solar energy. Materials 15(21):7507. https://doi.org/10.3390/ma15217507

Bilal A, Jamil B, Haque NU, Ansari MA (2019) Investigating the effect of pumice stones sensible heat storage on the performance of a solar still. Groundw Sustain Dev 9:100228. https://doi.org/10.1016/j.gsd.2019.100228

Darawsheh I, Islam MD, Banat F (2019) Experimental characterization of a solar powered MSF desalination process performance. Therm Sci Eng Prog 10:154–162. https://doi.org/10.1016/j.tsep.2019.01.018

Devarajan VP, Madhavan VR (2022) Experimental analysis of CO_2 reduction using low surface area carbon beads (CB) and Ca/CB catalyst by thermocatalytic gasification for fuel gas production. Biomass Conv Bioref 13:7319–7331. https://doi.org/10.1007/s13399-022-03358-4

El-Sebaii AA, Yaghmour SJ, Al-Hazmi FS, Faidah AS, Al-Marzouki FM, Al-Ghamdi AA (2009) Active single basin solar still with a sensible storage medium. Desalination 249(2):699–706. https://doi.org/10.1016/j.desal.2009.02.060

Faegh M, Shafii MB (2017) Experimental investigation of a solar still equipped with an external heat storage system using phase change materials and heat pipes. Desalination 409:128–135. https://doi.org/10.1016/j.desal.2017.01.023

Faghiri S, Mohammadi O, Hosseininaveh H, Shafii MB (2021) The impingement of liquid boiling droplet onto a molten phase change material as a direct-contact solidification method. Therm Sci Eng Prog 23:100888. https://doi.org/10.1016/j.tsep.2021.100888

Faghiri S, Aria HP, Shafii MB (2022) Multi-objective optimization of acetone droplet impingement on phase change material in direct-contact discharge method. J Energy Storage 46:103862. https://doi.org/10.1016/j.est.2021.103862

Faghiri S, Ahmadi R, Akbari S, Shafii MB (2023) Numerical analysis of latent thermal energy storage system under double spirally coiled tube configuration with two separated paths. Therm Sci Eng Prog 37:101585. https://doi.org/10.1016/j.tsep.2022.101585

Ghachem K, Selimefendigil F, Öztop HF, Almeshaal M, Alhadri M, Kolsi L (2021) Effects of magnetic field, binary particle loading and rotational conic surface on phase change process in a PCM filled cylinder. Case Stud Therm Eng 28:101456. https://doi.org/10.1016/j.csite.2021.101456

Haillot D, Pincemin S, Goetz V, Rousse DR, Py X (2017) Synthesis and characterization of multifunctional energy composite: solar absorber and latent heat storage material of high thermal conductivity. Sol Energy Mater Sol Cells 161:270–277. https://doi.org/10.1016/j.solmat.2016.12.010

Kabeel AE, Abdelgaied M (2016) Improving the performance of solar still by using PCM as a thermal storage medium under Egyptian conditions. Desalination 383:22–28. https://doi.org/10.1016/j.desal.2016.01.006

Kabeel AE, El-Agouz SA, Sathyamurthy R, Arunkumar T (2018a) Augmenting the productivity of solar still using jute cloth knitted with sand heat energy storage. Desalination 443:122–129. https://doi.org/10.1016/j.desal.2018.05.026

Kabeel AE, El-Samadony YAF, El-Maghlany WM (2018b) Comparative study on the solar still performance utilizing different PCM. Desalination 432:89–96. https://doi.org/10.1016/j.desal.2018.01.016

Kabeel AE, Harby K, Abdelgaied M, Eisa A (2020) Augmentation of a developed tubular solar still productivity using hybrid storage medium and CPC: an experimental approach. J Energy Storage 28:101203. https://doi.org/10.1016/j.est.2020.101203

Khan Z, Khan Z, Ghafoor A (2016) A review of performance enhancement of PCM based latent heat storage system within the context of materials, thermal stability and compatibility. Energy Convers Manage 115:132–158. https://doi.org/10.1016/j.enconman.2016.02.045

Panchabikesan K, Abaranji S, Vellaichamy P, Ramalingam V (2017) Effect of direct evaporative cooling during the charging process of phase change material-based storage system for building free cooling application—A real-time experimental investigation. Energy Build 152:250–263. https://doi.org/10.1016/j.enbuild.2017.07.037

Panchabikesan K, Swami MV, Panchabikesan K, Swami MV, Ramalingam V, Haghighat F (2019) Influence of PCM thermal conductivity and HTF velocity during solidification of PCM through the free cooling concept–a parametric study. J Energy Storage 21:48–57. https://doi.org/10.1016/j.est.2018.11.005

Radhwan AM (2005) Transient performance of a stepped solar still withbuilt-in latent heat thermal energy storage. Desalination 171(1):61–76. https://doi.org/10.1016/j.desa1.2003.12.010

Salah AH, Hassan GE, Fath H, Elhelw M, Elsherbiny S (2017) Analytical investigation of different operational scenarios of a novel greenhouse combined with solar stills. Appl Therm Eng 122:297–310. https://doi.org/10.1016/j.applthermaleng.2017.05.022

Selimefendigil F, Öztop HF (2022) Impacts of using an elastic fin on the phase change process under magnetic field during hybrid nanoliquid convection through a PCM-packed bed system. Int J Mech Sci 216:106958. https://doi.org/10.1016/j.ijmecsci.2021.106958

Vasu A, Hagos FY, Noor MM, Mamat R, Azmi WH, Abdullah AA, Ibrahim TK (2017) Corrosion effect of phase change materials in solar thermal energy storage application. Renew Sustain Energy Rev 76:19–33. https://doi.org/10.1016/j.rser.2017.03.018

Velraj RVSR, Seeniraj RV, Hafner B, Faber C, Schwarzer K (1999) Heat transfer enhancement in a latent heat storage system. Sol Energy 65(3):171–180. https://doi.org/10.1016/S0038-092X(98)00128-5

Vigneswaran VS, Kumaresan G, Elansezhiyan S, Velraj R (2019) Heat transfer studies on solar still assisted with and without latent heat storage material. Desalin Water Treat 140:1–6. https://doi.org/10.5004/dwt.2019.23314

Yousef MS, Hassan H (2019) Energetic and exergetic performance assessment of the inclusion of phase change materials (PCM) in a solar distillation system. Energy Convers Manage 179:349–361. https://doi.org/10.1016/j.enconman.2018.10.078

Publisher's note Springer Nature remains neutral with regard to jurisdictional claims in published maps and institutional affiliations.

Springer Nature or its licensor (e.g. a society or other partner) holds exclusive rights to this article under a publishing agreement with the author(s) or other rightsholder(s); author self-archiving of the accepted manuscript version of this article is solely governed by the terms of such publishing agreement and applicable law.